

热处理工艺对超音速火焰喷涂 Al-Cu-Fe 准晶涂层性能影响

万鹏¹, 曹达华¹, 周瑜杰¹, 杨玲¹, 辛先峰², 董闯²

(1. 佛山市顺德区美的电热电器制造有限公司, 广东 佛山 528300;

2. 大连理工大学, 辽宁 大连 116024)

摘要: **目的** 使用超音速火焰喷涂 (HVOF) 方法制备 Al-Cu-Fe 准晶涂层, 研究热处理温度对涂层中准晶相含量和性能的影响以及封孔处理对涂层耐蚀性的改善。**方法** 以 304 不锈钢为基体和真空雾化 Al-Cu-Fe 准晶粉末为热喷涂材料, 采用超音速火焰喷涂方法制备准晶涂层, 并进行 550~700 °C 热处理。利用透射电镜、扫描电镜、光学显微镜、能谱分析仪和 X 射线衍射仪分析准晶粉末和涂层的衍射花样、微观形貌、成分和相结构。分别使用显微硬度仪和电化学工作站对比测量 304 不锈钢和准晶涂层的硬度和耐蚀性能。**结果** 粉末中二十面体准晶相 (I 相) 为主相, 并伴生准晶类似相 (β 相)。经过超音速火焰喷涂后, 涂层中 I 相和 β 相的含量分别为 78.7% 和 21.3%, 相组成与原始粉末接近。550 °C 和 600 °C 热处理 1 h 后, 涂层中 β 相消失, I 相占比进一步上升, 并伴随 Al_2Cu (θ 相) 产生。随着热处理温度继续升高至 650 °C, β 相开始重新析出; 当热处理温度升至 700 °C, β 相占比增至 13.5%。热处理后准晶涂层的最高硬度为 674HV, 为 304 不锈钢硬度 (182HV) 的 3.7 倍。准晶涂层经过热处理和表面封孔后, 其在 3.5%NaCl 溶液中腐蚀的速率低于 304 不锈钢。**结论** 合适的热处理温度是制备高纯准晶涂层的关键因素, 准晶含量的提升有利于提高准晶涂层的硬度和耐蚀性。

关键词: 准晶涂层; 超音速火焰喷涂; 热处理; 相组成; 硬度; 腐蚀

中图分类号: TG174.442 文献标识码: A 文章编号: 1001-3660(2023)02-0422-08

DOI: 10.16490/j.cnki.issn.1001-3660.2023.02.041

Impact of Annealing Treatment on the Properties of High-velocity Oxy-fuel Sprayed Al-Cu-Fe Quasi-crystalline Coating

WAN Peng¹, CAO Da-hua¹, ZHOU Yu-jie¹, YANG Ling¹, XIN Xian-feng², DONG Chuang²

(1. Foshan Shunde Midea Electrical Heating Appliances Manufacturing Co., Ltd., Guangdong Foshan 528300, China;

2. Dalian University of Technology, Liaoning Dalian 116024, China)

ABSTRACT: Quasi-crystals, being brittle and porous in bulk form, are usually prepared as coatings, especially using thermal spraying for practical applications. However, due to the strict requirements for the formation of quasi-crystalline

收稿日期: 2022-01-07; 修订日期: 2022-04-02

Received: 2022-01-07; Revised: 2022-04-02

基金项目: 顺德区科技计划项目 (201911220001)

Fund: Shunde District Science and Technology Project (201911220001)

作者简介: 万鹏 (1990—), 男, 博士, 主要研究方向为表面工程。

Biography: WAN Peng (1990-), Male, Doctor, Research focus: surface engineering.

引文格式: 万鹏, 曹达华, 周瑜杰, 等. 热处理工艺对超音速火焰喷涂 Al-Cu-Fe 准晶涂层性能影响[J]. 表面技术, 2023, 52(2): 422-429.

WAN Peng, CAO Da-hua, ZHOU Yu-jie, et al. Impact of Annealing Treatment on the Properties of High-velocity Oxy-fuel Sprayed Al-Cu-Fe Quasi-crystalline Coating[J]. Surface Technology, 2023, 52(2): 422-429.

phases, powder composition, oxidization, spraying parameter, and heat treatment condition are all involved, which makes the preparation of high purity quasi-crystalline coatings quite difficult. Among the many thermal spraying techniques, high-velocity oxy-fuel spraying (HVOF) should be a good choice for such a purpose as it has a low heat-source temperature and a high particle projection speed, which can effectively avoid the oxidation of quasi-crystalline particles, reduce the ablation of the component metals of quasi-crystalline alloys, and improve the compactness and bonding strength of the coatings. In this article, high purity quasi-crystalline coatings are prepared using HVOF process. Besides the spraying process, heat treatments are specially focused to unveil the effects of different post-annealings on the content of quasi-crystalline phase, microstructure, hardness, and corrosion resistance of the prepared coatings.

The chemical composition $\text{Al}_{63}\text{Cu}_{25}\text{Fe}_{12}$ of the icosahedral quasicrystal in Al-Cu-Fe system is first selected according to the cluster-plus-glue-atom model and the electron-per-atom ratio (e/a), $e/a=1.86$. The pure Al, Cu and Fe metals are then melted into ingots in a vacuum induction furnace and the ingots are further atomized to make powders with particle size in the range of 15-50 μm , the average particle size with high sphericity is 25 μm . Lijia HV-8000 HVOF system is adopted to prepare quasi-crystalline coatings. The spraying parameters are as follows: the speed of spray gun is 300 mm/s, the spraying distance is 300 mm, the flow rate of aviation kerosene is 19 L/h, the flow rate of oxygen is 1 850 scfh (1 scfh=28.3 L/h), and the powder feed rate is 30-35 g/min. The as-deposited coatings are finally annealed at 550-700 $^{\circ}\text{C}$ for 1 hour in argon atmosphere. The surface of annealed sample is immersed in the sealing agent for 5 min and then cured at 380 $^{\circ}\text{C}$ for 10 min. FEI Talos F200X transmission electron microscopy (TEM) is used to characterize the diffraction patterns. Hitachi TM4000 plus scanning electron microscopy (SEM), energy dispersive spectroscopy (EDS) and ZEISS optical microscope are used to observe the microstructure and composition, respectively. Smartlab SE X-ray diffractometer (XRD) is used for phase analysis. The bonding strength is measured by MTS universal tensile testing machine. The hardness is measured by WilsonVH1202 microhardness tester. The electrochemical workstation is used to measure the corrosion resistance in 3.5wt.% NaCl solution.

Icosahedral quasi-crystal phase (I phase) is the main phase (about 77%) of the powder, as evidenced by five-fold diffraction patterns, accompanied by approximant phase β . After HVOF deposition, I phase and β phase of the as-deposited coating are 78.7% and 21.3%, respectively. The thickness of the coating is 330 μm and the bonding strength is 36 MPa. After heat treatments at 550 $^{\circ}\text{C}$ and 600 $^{\circ}\text{C}$ for 1 hour, β phase disappears and the proportion of I phase increases further, accompanied by the formation of Al_2Cu (θ phase). After heat treatments at 650 $^{\circ}\text{C}$ for 1 hour, β phase precipitates again. When the heat treatment temperature rises to 700 $^{\circ}\text{C}$, β phase proportion increases to 13.5%. After heat treatments, the highest hardness of the quasi-crystalline coating is 674HV, which is 3.7 times that of 304 stainless steel (182HV). The corrosion rate in NaCl solution of the quasi-crystalline coating after heat treatment and surface sealing is lower than that of 304 stainless steel.

In summary, high purity quasi-crystalline coatings with high compactness and good bonding strength can be prepared by high-velocity oxy-fuel spraying. Proper heat treatment temperature is the key factor to obtain high purity quasi-crystalline phase. The increase of quasi-crystalline content is beneficial to improve the hardness and corrosion resistance of the coatings.

KEY WORDS: quasi-crystalline coating; high velocity oxy-fuel spraying; heat treatment; phase structure; hardness; corrosion

准晶 (Quasi-crystals) 是一类同时具有长程有序原子排列和非晶体学旋转对称性的金属间化合物^[1-3], 呈现出一系列介于金属与化合物之间独特的性能, 如高硬度^[4]、低摩擦因数^[5-6]、高耐磨性^[7-8]、低表面能^[9]和低导热率^[10]等, 在耐磨、隔热和防黏等领域有着巨大的应用潜力。但准晶同时具有常温脆性和疏松的特点, 在实际应用中为解决这一难题并发挥其性能优势, 一般采用在特定基体上制备准晶薄膜或涂层^[11-13]。常用的准晶薄膜或涂层制备工艺为物理气相沉积 (PVD)^[14-16]和热喷涂^[17-18]。PVD 工艺

制备的薄膜一般厚度较薄且沉积速率低; 而热喷涂工艺可以获得较厚涂层, 并与基体具有良好的结合力, 且喷涂面积大、沉积速率高^[19]。热喷涂根据热源的不同分为火焰喷涂、电弧喷涂和等离子喷涂。其中, 超音速火焰喷涂 (HVOF) 采用航空煤油、丙烯、氢气等作为燃料, 与助燃剂氧气在燃烧室燃烧并产生超音速高温焰流, 将喷涂粒子加热至熔化或半熔化状态, 获得结合强度高、致密性好的优质涂层^[20-21]。与等离子喷涂相比, HVOF 喷涂热源温度更低, 可以有效防止准晶颗粒氧化及准晶态合金组元

的烧蚀, 利于制备高纯度准晶涂层^[22]; 同时, HVOF 喷涂粒子速度更快, 利于提升准晶涂层的致密性和结合力。

当前准晶涂层研究和应用仍面临两个突出问题: 一方面由于准晶相的形成条件要求严格, 在准晶涂层制备过程中, 喷涂粉末成分偏移、喷涂工艺或基材选择不当等因素会导致准晶相转变为准晶类似相和其他晶体相, 进而影响涂层性能^[23-24]。傅迎庆等^[25]采用爆炸喷涂制备了 Al-Cu-Cr 准晶涂层, 当喷涂能量增加时, 利于获得高硬度的致密涂层, 但也会引发低熔点合金组元 Al 的氧化烧损加剧, 涂层中类似相比比例增加, 准晶相比比例降低。另一方面, 热喷涂涂层是由扁平化熔融粒子搭界而成, 涂层表面不可避免地存在一定的孔隙^[26]。通常情况下, 随着涂层孔隙率的增加, 其耐蚀性能下降^[27]。本文采用 HVOF 工艺制备 Al-Cu-Fe 准晶涂层, 一方面通过热处理工艺提升涂层中的准晶相比比例, 另一方面采用表面封孔的方式改善涂层的耐蚀性能, 并研究了准晶涂层中物相、微观组织及涂层硬度、电化学性能随热处理温度的变化规律。

1 试验

1.1 成分设计和粉末制备

根据“团簇加连接原子”模型设计理论, 选用 $e/a=1.86$ 的 [Al-Cu-Fe] 二十面体结构成分, 即原子比 $Al_{63}Cu_{25}Fe_{12}$ 成分^[28]。采用雾化法制粉, 将 Al、Cu 和 Fe 纯料按比例配制好, 放入真空感应炼炉中熔炼合金铸锭, 再将锭子放入雾化设备中加热, 在保护气氛下, 将铸锭加热到熔融状态, 利用气体压力将熔融态的准晶合金制成粉末。利用机械振动筛筛分出粒度为 15~50 μm 的 Al-Cu-Fe 合金粉末, 用于超音速火焰喷涂。

1.2 材料及涂层制备

试样基体选用 304 不锈钢材料, 先对基体除油、除锈, 确保基体表面无污染, 然后再用刚玉颗粒对基体进行喷砂处理, 增加基体表面粗糙度。采用郑州立佳超音速火焰喷涂系统 HV-8000, 该系统使用航空煤油为燃料, 在喷枪的燃烧室与氧气混合燃烧, 经拉瓦尔喷嘴加速后, 形成超音速火焰束流。送粉器在氮气压力下将准晶合金粉末送入燃烧室, 粉末颗粒被加热至熔化或半熔化状态, 并加速喷射到基体上沉积成致密的涂层结构。喷涂参数如表 1 所示。采用氩气气氛的热处理炉, 热处理温度为 550~700 $^{\circ}C$, 保温时间为 1 h。封孔剂采用氟树脂乳液, 将样品表面浸没于封孔剂中 5 min 后进行表面干燥, 再经过 380 $^{\circ}C$ 保温 10 min 进行固化烧结。

表 1 超音速火焰喷涂 Al-Cu-Fe 准晶涂层工艺参数
Tab.1 High-velocity oxy-fuel spraying parameters for Al-Cu-Fe quasi-crystalline coatings

No.	Parameters	Value
1	Traverse speed/(mm·s ⁻¹)	300
2	Spray distance/mm	300
3	Spray angle/($^{\circ}$)	90
4	Kerosene flow rate/(L·h ⁻¹)	19
5	Oxygen flow rate scfh (1 scfh=28.3 L/h)	1 850
6	Powder feed rate/(g·min ⁻¹)	30-35

1.3 性能表征

采用 FEI Talos F200X 型透射电镜 (TEM) 对粉末和涂层的衍射花样进行表征。采用日立 TM4000plus 扫描电镜 (SEM)、能谱分析仪 (EDS) 及 ZEISS Axioscope A1 光学显微镜观察粉末和涂层的微观形貌及成分分析。采用日本理学 Smartlab SE 型 X 射线衍射仪 (XRD) 进行物相分析。利用 MTS 万能拉伸试验机进行拉伸试验, 按照 GB/T 8642《热喷涂抗拉结合强度的测定》进行测定涂层与基体的结合强度。采用 WilsonVH1202 维式显微硬度仪测量涂层硬度, 随机选取样品表面 5 个位置进行测试, 采用 0.2 kg 载荷和顶角为 136 $^{\circ}$ 的金刚石方形锥压入材料表面并保压 30 s, 用载荷值除以材料压痕凹坑的面积得到维氏硬度值。采用电化学工作站测量涂层和基材的耐蚀性能, 电解质为 3.5%NaCl 溶液。

2 结果与分析

2.1 粉末分析

雾化法制备的 Al-Cu-Fe 准晶粉末表面形貌的 SEM 照片如图 1 所示。经过统计, 粉末粒径范围为 15~50 μm , 平均粒径为 25 μm , 粉末球形度高, 利于提高超音速火焰喷涂时粉末的流动性。由于雾化过程中冷却速度不同, 准晶合金粉末的表面含少量的卫星颗粒^[17]。

图 2 为超音速火焰喷涂所采用 Al-Cu-Fe 准晶粉末的 XRD 图谱, 从图中可知准晶粉末中二十面体准晶相 (I 相) 为主相, 并伴生准晶类似相 (β 相)。通过统计 I 相和 β 相的衍射峰面积占比, 计算得到准晶粉末中 I 相的含量为 77%, β 相的含量为 23%。图 3a 和图 3b 分别为 Al-Cu-Fe 准晶粉末的 TEM 明场像和衍射图, 粉末的衍射斑点具有 5 次对称的非晶体学旋转对称的特性, 进一步证明了粉末中含有二十面体准晶结构。

2.2 涂层分析

图 4 为超音速火焰喷涂制备的 Al-Cu-Fe 准晶涂

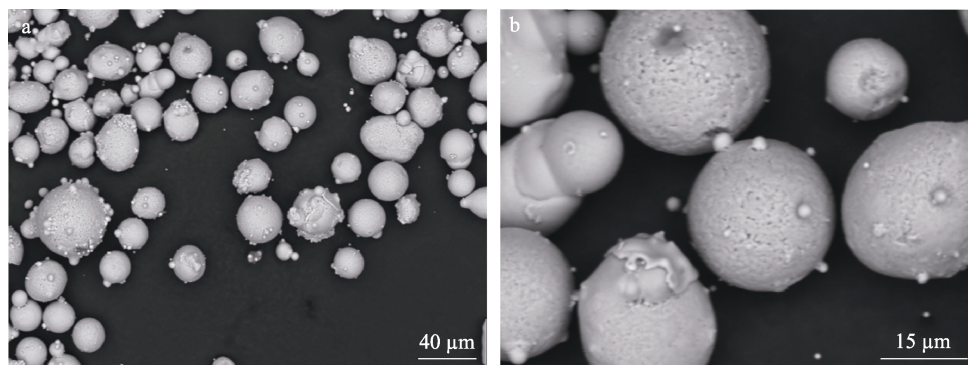


图 1 Al-Cu-Fe 准晶粉末的 SEM 照片

Fig.1 SEM images of surface morphology for Al-Cu-Fe quasi-crystalline powders

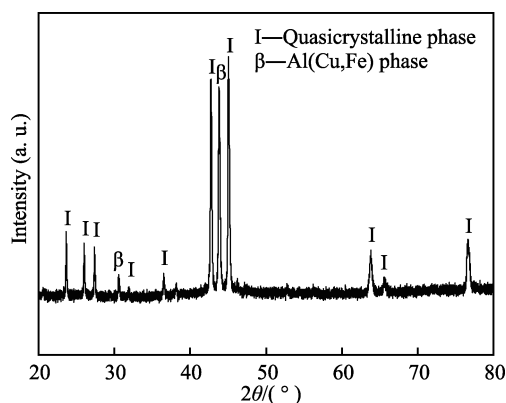


图 2 Al-Cu-Fe 准晶粉末的 XRD 图谱

Fig.2 XRD patterns of Al-Cu-Fe quasi-crystalline powders

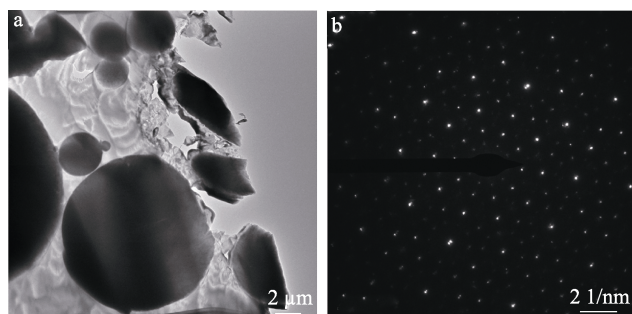


图 3 Al-Cu-Fe 准晶粉末 TEM 明场像 (a) 和衍射图 (b)

Fig.3 The TEM image (a) and diffraction patterns (b) of Al-Cu-Fe quasi-crystalline powders

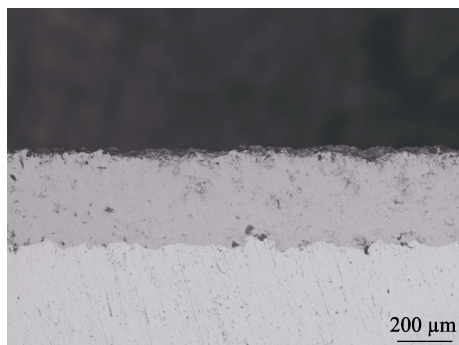


图 4 Al-Cu-Fe 准晶涂层的截面微观形貌

Fig.4 SEM image of cross-section microstructures for Al-Cu-Fe quasi-crystalline coating

层截面微观形貌, 涂层厚度为 330 μm , 涂层无裂纹但含有一定量的孔隙。形成 Al-Cu-Fe 涂层孔隙的原因主要有两个: (1) 超音速火焰喷涂过程中, 准晶粒子经过高温变形、相互交错和堆积而成的层状结构, 由于粒子变形不充分, 在堆叠过程中形成孔隙^[26]; (2) 采用 EDS 元素分析, Al、Cu 和 Fe 的平均原子数分数分别为 60.2%、25.5%和 14.3%, 基本符合设计成分 ($\text{Al}_{63}\text{Cu}_{25}\text{Fe}_{12}$), 其中 Al 的烧蚀为 4%左右。由于 Al 元素的熔点低, 在高温焰流下部分气化, 当气体来不及从粒子内逸出时, 在涂层内部形成孔隙。

采用拉伸试验机, 对黏直径 25 mm 的准晶涂层样品, 测得涂层的抗拉力为 17 607 N, 换算得到准晶涂层的结合力为 36 MPa。文献研究表明^[28], 准晶材料的室温脆性在高温下完全消失, 具有类似于超塑性的极高塑性。超音速火焰喷涂先将准晶粒子加热至熔融或半熔融状态, 再以数倍音速的速度撞击到喷砂处理的基材上, 形成高强度机械结合。

2.3 涂层热处理

图 5 为准晶涂层经不同温度热处理后的 XRD 图谱, 并计算准晶涂层中各个晶相的比例, 如表 2 所示。

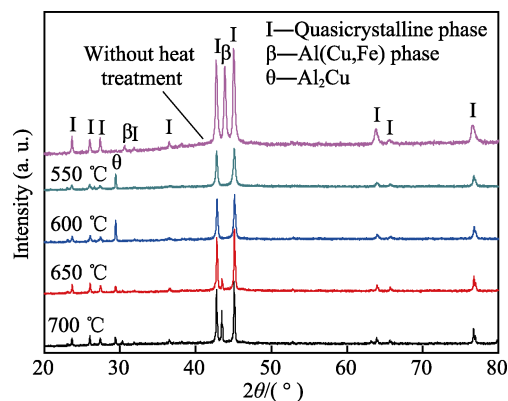


图 5 准晶涂层未热处理及经过不同温度热处理后的 XRD 图谱

Fig.5 XRD patterns of quasi-crystalline coatings without heat treatment and after heat treatment at different temperatures

表 2 不同温度热处理后准晶涂层中 I、 β 和 θ 的含量
Tab.2 The relative amount of I, β and θ phases for quasi-crystalline coatings annealed at different temperatures

Phase	mol. %				
	RT	550 °C	600 °C	650 °C	700 °C
I	78.7	92.9	90.2	93.5	83.5
β	21.3	0	0	3.6	13.5
θ	0	7.1	9.8	2.9	3.0

未热处理的涂层中 I 相占比为 78.7%， β 相占比为 21.3%，涂层的相组成与原始粉末接近。经过 550 °C 和 600 °C 热处理后，涂层中 β 相消失，I 相占比进一步上升，并伴随 Al_2Cu (θ 相) 产生。随着热处理温度继续升高至 650 °C， β 相开始重新析出；当热处理温度升至 700 °C， β 相占比增至 13.5%。说明超音速火焰喷涂制备的 Al-Cu-Fe 准晶涂层形成准晶相的最佳热处理条件为 550~650 °C，在此温度区间内准晶涂层中二十面体准晶相占比高于 90%。

图 6 为 600 °C 热处理后的 Al-Cu-Fe 涂层的 TEM 明场像 (图 6a) 和衍射图 (图 6b)，此区域的衍射斑点具有准晶的 5 次对称特征，表明涂层中含有二十面

体准晶相。

图 7 为热处理前后准晶涂层的表面形貌。可以看出，未热处理的准晶涂层 (图 7a) 中大孔 (图中箭头所示) 的孔径为 30~40 μm ；600 °C 热处理后准晶涂层 (图 7b) 中大孔 (图中箭头所示) 的孔径降至 15~25 μm ，同时涂层的孔隙率有所降低，说明热处理过程中准晶涂层发生致密化过程。

2.4 涂层性能表征

图 8 为 304 不锈钢和准晶涂层的维氏硬度对比，其中 304 不锈钢的硬度为 182HV，未热处理准晶涂层的硬度为 487HV，未热处理准晶涂层的硬度是 304 不锈钢的 2.6 倍。这是由于准晶材料的力学性能与金属间化合物类似，其结合键除具有金属键外，还有较强的共价键成分，因此硬度比 304 不锈钢高。经过 550~650 °C 热处理后，准晶涂层的硬度为 586~674HV，此时涂层中 I 相占比大于 90%；而随着热处理温度继续增加至 700 °C，准晶涂层的硬度下降至 555HV，此时准晶涂层中 β 相不断增加，I 相占比下降。结果表明，消除准晶涂层中的 β 相有利于提高涂层硬度。

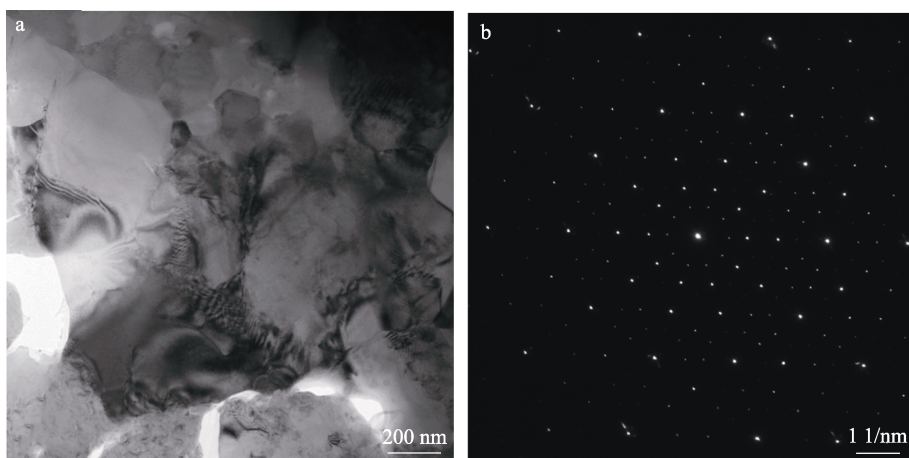


图 6 600 °C 热处理后的 Al-Cu-Fe 涂层 TEM 明场像 (a) 和衍射图 (b)

Fig.6 The TEM image (a) and diffraction patterns (b) of Al-Cu-Fe coatings after heat treatment at 600 °C

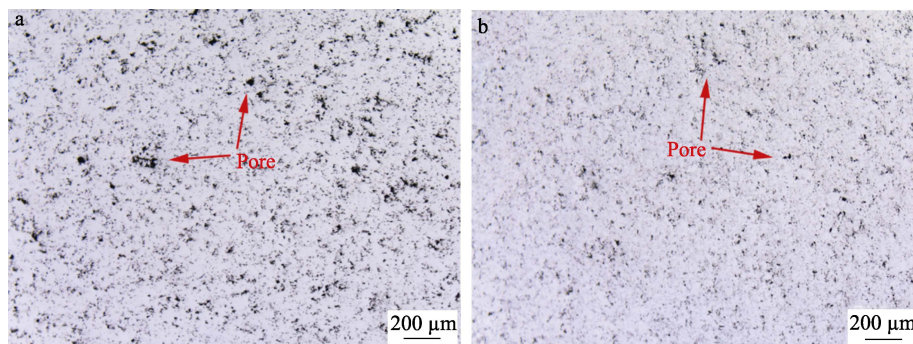


图 7 准晶涂层未热处理 (a) 和 600 °C 热处理后 (b) 的表面形貌

Fig.7 Surface morphology of quasi-crystalline coatings without heat treatment (a) and after heat treatment at 600 °C (b)

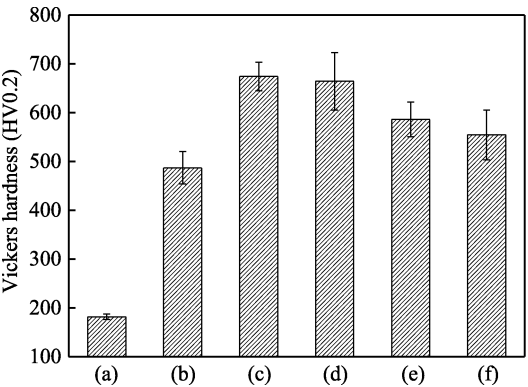


图 8 304 不锈钢 (a)、未热处理 (b) 及 550 °C (c)、600 °C (d)、650 °C (e)、700 °C (f) 热处理后的准晶涂层的维氏硬度

Fig.8 Vickers hardness of 304 stainless steel (a), quasi-crystalline coatings without heat treatment (b) and after heat treatment at different temperatures 550 °C (b), 600 °C (c), 650 °C (d) and 700 °C (e), respectively

表 3 为 304 不锈钢与不同工艺热处理后的准晶涂层的耐蚀性对比, 其中 J_{corr} 为材料在 3.5%NaCl 溶液中的自腐蚀电流密度。从表 3 可知, 304 不锈钢的自腐蚀电流密度为 $1.39 \times 10^{-6} \text{ A/cm}^2$, 而未热处理的准晶涂层的自腐蚀电流密度为 $1.69 \times 10^{-5} \text{ A/cm}^2$ 。表明未热处理的准晶涂层的耐蚀性远低于 304 不锈钢, 一方面是由于涂层存在准晶相 (I 相) 和准晶类似相 (β 相) 形成电偶腐蚀; 另一方面是涂层中存在孔隙, NaCl 溶液中的 Cl^- 具有离子半径小、穿透能力强的特点, 会优先从孔隙中侵入, 加速涂层腐蚀。热处理后的准晶涂层的自腐蚀电流密度为 $2.26 \times 10^{-6} \text{ A/cm}^2$, 比未热处理的准晶涂层降低了 1 个数量级, 表明涂层的耐蚀性明显提升。原因有两点: (1) 准晶涂层中 I 相占比从 78.7% (未热处理) 提升至 90.2% (600 °C 热处理), 降低了 I 相与杂质相之间电偶腐蚀的影响; (2) 热处理后准晶涂层的孔隙率降低、致密度增加, 有效减少了孔隙腐蚀。由于热处理无法完全消除涂层中的孔隙, 为了进一步提高准晶涂层的耐蚀性,

表 3 304 不锈钢与不同工艺热处理的准晶涂层的耐蚀性对比

Tab.3 Corrosion resistance comparison between 304 stainless steel and quasi-crystalline coatings with different post-treatment parameters

Specimen number	Sample information	Post-treatment parameters	$J_{\text{corr}}/(\text{A} \cdot \text{cm}^{-2})$
S1	304 stainless steel		1.39×10^{-6}
S2			1.69×10^{-5}
S3	Quasi-crystalline coatings	Heat treatment (600 °C)	2.26×10^{-6}
S4		Heat treatment (600 °C) and sealing treatment	1.07×10^{-6}

采用氟树脂涂料对热处理后的准晶涂层表面进行封孔处理, 经测试涂层的自腐蚀电流密度降低至 $1.07 \times 10^{-6} \text{ A/cm}^2$, 表明其在 3.5%NaCl 溶液中的腐蚀速率低于 304 不锈钢。

3 结论

- 1) 真空雾化制备的准晶粉末中二十面体准晶相 (I 相) 为主相, 并伴生准晶类似相 (β 相)。
- 2) 经过超音速火焰喷涂后, 涂层中 I 相和 β 相的含量分别为 78.7%和 21.3%, 相组成与原始粉末接近。550 °C和 600 °C热处理 1 h 后, 涂层中 β 相消失, I 相占比进一步上升, 并伴随 Al_2Cu (θ 相) 产生。随着热处理温度继续升高至 650 °C, β 相开始重新析出; 当热处理温度升至 700 °C, β 相占比增至 13.5%。
- 3) 未热处理准晶涂层的硬度为 487HV, 550~700 °C热处理后准晶涂层的最高硬度为 674HV, 是 304 不锈钢硬度 (182HV) 的 3.7 倍。准晶 I 相硬度高于 β 相, 消除准晶涂层中的 β 相有利于提高涂层硬度。
- 4) 600 °C热处理的准晶涂层的自腐蚀电流密度比未热处理的准晶涂层降低了 1 个数量级, 而且经过进一步表面封孔处理后, 其在 3.5%NaCl 溶液中的腐蚀速率低于 304 不锈钢。

参考文献:

[1] SHECHTMAN D, BLECH I, GRATIAS D, et al. Metallic Phase with Long-Range Orientational Order and no Translational Symmetry[J]. Physical Review Letters, 1984, 53(20): 1951-1953.

[2] ELSER V V. Comment on Quasicrystals: A New Class of Ordered Structures[J]. Physical Review Letters, 1985, 54(15): 1730.

[3] 董闯, 王英敏, 姜建兵, 等. 准晶: 奇特而又平凡的晶体——2011 年诺贝尔化学奖简介[J]. 自然杂志, 2011, 33(6): 322-327, 377.

DONG Chuang, WANG Ying-min, QIANG Jian-bing, et al. Quasi-Periodic Crystals: Exotic but Common—A Brief Introduction to the Nobel Prize in Chemistry 2011[J]. Chinese Journal of Nature, 2011, 33(6): 322-327, 377.

[4] LEPESHEV A A, ROZHKOVA E A, KARPOV I V, et al. Physical, Mechanical, and Tribological Properties of Quasicrystalline Al-Cu-Fe Coatings Prepared by Plasma Spraying[J]. Physics of the Solid State, 2013, 55(12): 2531-2536.

[5] BRUNET P, ZHANG L M, SORDELET D J, et al. Comparative Study of Microstructural and Tribological Properties of Sintered, Bulk Icosahedral Samples[J]. Materials Science and Engineering: A, 2000, 294-296: 74-78.

[6] YADAV T, MUKHOPADHYAY N. Quasicrystal: A Low-

- Frictional Novel Material[J]. *Current Opinion in Chemical Engineering*, 2018, 19: 163-169.
- [7] SALES M, MERSTALLINGER A, USTINOV A I, et al. Effect of the Addition of Crystalline B-Phase in Al-Cu-Fe Quasicrystalline Coatings on Their Tribological Properties[J]. *Surface and Coatings Technology*, 2007, 201(14): 6206-6211.
- [8] DUBOIS J M, BRUNET P, COSTIN W, et al. Friction and Fretting on Quasicrystals under Vacuum[J]. *Journal of Non-Crystalline Solids*, 2004, 334-335: 475-480.
- [9] DUBOIS J M. New Prospects from Potential Applications of Quasicrystalline Materials[J]. *Materials Science and Engineering: A*, 2000, 294-296: 4-9.
- [10] 王全胜, 李和章, 李佳彬, 等. 等离子喷涂 AlCuCoSi 准晶热障涂层性能研究[J]. *热喷涂技术*, 2009, 1(1): 30-33.
- WANG Quan-sheng, LI He-zhang, LI Jia-bin, et al. Study on Properties of AlCuCoSi Quasicrystal TBCS by APS[J]. *Thermal Spray Technology*, 2009, 1(1): 30-33.
- [11] 周细应, 徐洲. Al-Cu-Fe 准晶薄膜/涂层的研究进展[J]. *热加工工艺*, 2009, 38(2): 82-86, 139.
- ZHOU Xi-ying, XU Zhou. Research Progress of Al-Cu-Fe Quasicrystalline Films/Coatings[J]. *Hot Working Technology*, 2009, 38(2): 82-86, 139.
- [12] 辛先峰, 董闯, 庞厂, 等. 涂层和薄膜态准晶材料的研究现状及展望[J]. *表面技术*, 2020, 49(5): 19-25.
- XIN Xian-feng, DONG Chuang, PANG Chang, et al. State-of-the-Art and Prospects of Quasicrystalline Coatings and Thin Films[J]. *Surface Technology*, 2020, 49(5): 19-25.
- [13] 钟嘉彬, 陈永君, 滕琳琳, 等. Al 基准晶薄膜/涂层研究进展[J]. *中国表面工程*, 2021, 34(5): 105-116.
- ZHONG Jia-bin, CHEN Yong-jun, TENG Lin-lin, et al. Research Progress on Al-Based Quasicrystal Films/Coatings[J]. *China Surface Engineering*, 2021, 34(5): 105-116.
- [14] DANIELS M J, KING D, FEHRENBACHER L, et al. Physical Vapor Deposition Route for Production of Al-Cu-Fe-Cr and Al-Cu-Fe Quasicrystalline and Approximant Coatings[J]. *Surface and Coatings Technology*, 2005, 191(1): 96-101.
- [15] POLISHCHUK S, BOULET P, MÉZIN A, et al. Residual Stress in As-Deposited Al-Cu-Fe-B Quasicrystalline Thin Films[J]. *Journal of Materials Research*, 2012, 27(5): 837-844.
- [16] YADAV T P, SINGH D, SHAHI R R, et al. Synthesis of Quasicrystalline Film of Al-Ga-Pd-Mn Alloy[J]. *Thin Solid Films*, 2013, 534: 265-269.
- [17] 蔡明伟, 曲寿江, 魏先顺, 等. 喷涂工艺对超音速火焰喷涂 Al-Cu-Fe-Si 准晶合金涂层性能的影响[J]. *表面技术*, 2016, 45(2): 73-78.
- CAI Ming-wei, QU Shou-jiang, WEI Xian-shun, et al. Effect of Spraying Technology on the Properties of AC-HVAF Sprayed Al-Cu-Fe-Si Quasicrystalline Alloy Coating[J]. *Surface Technology*, 2016, 45(2): 73-78.
- [18] 张忠明, 冯亚如, 徐春杰, 等. 等离子喷涂 Al₆₅Cu₂₃Fe₁₂ 涂层的组织与性能研究[J]. *兵器材料科学与工程*, 2008, 31(1): 23-26.
- ZHANG Zhong-ming, FENG Ya-ru, XU Chun-jie. Microstructure and Property of Al₆₅Cu₂₃Fe₁₂ Coating Prepared by Plasma Spraying[J]. *Ordnance Material Science and Engineering*, 2008, 31(1): 23-26.
- [19] PARSAMEHR H, CHEN Tai-sheng, WANG D S, et al. Thermal Spray Coating of Al-Cu-Fe Quasicrystals: Dynamic Observations and Surface Properties[J]. *Materialia*, 2019, 8: 100432.
- [20] 周克崧, 刘敏, 邓春明, 等. 新型热喷涂及其复合技术的进展[J]. *中国材料进展*, 2009, 28(S2): 1-8.
- ZHOU Ke-song, LIU Min, DENG Chun-ming, et al. Recent Development of New Thermal Spray Technology and Combined Technology[J]. *Materials China*, 2009, 28(S2): 1-8.
- [21] 邝宣科, 钱士强. 超音速火焰喷涂涂层耐磨性能研究进展[J]. *上海工程技术大学学报*, 2010, 24(4): 363-366.
- KUANG Xuan-ke, QIAN Shi-qiang. Research Progress of Wear Resistance of High Velocity Oxy-Fuel Spraying Coating[J]. *Journal of Shanghai University of Engineering Science*, 2010, 24(4): 363-366.
- [22] 傅迎庆, 周锋, 高阳, 等. 超音速火焰喷涂 Al-Cu-Cr 准晶涂层表面不黏性和耐磨性的研究[J]. *稀有金属材料与工程*, 2009, 38(S2): 635-639.
- FU Ying-qing, ZHOU Feng, GAO Yang, et al. Surface Non-Sticking and Wear-Resisting Properties of High-Velocity Oxy-Fuel Sprayed Al-Cu-Cr Quasicrystalline Coatings[J]. *Rare Metal Materials and Engineering*, 2009, 38(S2): 635-639.
- [23] LEE K, CHEN Yan, DAI Wei, et al. Design of Quasicrystal Alloys with Favorable Tribological Performance in View of Microstructure and Mechanical Properties[J]. *Materials & Design*, 2020, 193: 108735.
- [24] 傅迎庆, 任仲兴, 梁志强, 等. 基体热导率对超音速火焰喷涂 Al-Cu-Cr 准晶涂层相组成的影响[J]. *大连海事大学学报*, 2008, 34(1): 112-115.
- FU Ying-qing, REN Zhong-xing, LIANG Zhi-qiang, et al. Influence of Substrate Thermal Conductivity on the Phase Composition of High Velocity Oxy-Fuel Sprayed Al-Cu-Cr Quasicrystalline Coatings[J]. *Journal of Dalian Maritime University*, 2008, 34(1): 112-115.
- [25] 傅迎庆, 周锋, 张立志, 等. 爆炸喷涂 Al-Cu-Cr 准晶涂层的组织及硬度研究[J]. *材料热处理学报*, 2007, 28(S1): 193-197.

- FU Ying-qing, ZHOU Feng, ZHANG Li-zhi, et al. Microstructure and Hardness Properties of Detonation Spraying Al-Cu-Cr Quasicrystalline Coatings[J]. Transactions of Materials and Heat Treatment, 2007, 28(S1): 193-197.
- [26] 姜超平, 王军兴, 张晓琳. 热喷涂制备 Fe 基非晶态合金涂层研究进展[J]. 热加工工艺, 2016, 45(22): 38-42.
- JIANG Chao-ping, WANG Jun-xing, ZHANG Xiao-lin. Research Progress of Fe Matrix Amorphous Coating Prepared by Thermal Spraying[J]. Hot Working Technology, 2016, 45(22): 38-42.
- [27] 靳子昂, 朱丽娜, 刘明, 等. 热喷涂技术制备铝涂层及其在 3.5%NaCl 溶液中耐腐蚀性的研究现状[J]. 表面技术, 2019, 48(10): 220-229.
- JIN Zi-ang, ZHU Li-na, LIU Ming, et al. Research Status of Aluminum Coating Prepared by Thermal Spraying Technology and Its Corrosion Resistance in 3.5% NaCl Solution[J]. Surface Technology, 2019, 48(10): 220-229.
- [28] 董闯. 准晶材料[M]. 北京: 国防工业出版社, 1998.
- DONG Chuang. Quasicrystalline Materials[M]. Beijing: National Defense Industry Press, 1998.
- 责任编辑: 万长清

(上接第 411 页)

- [23] XIE Ying-chun, CHEN Chao-yue, PLANCHE M P, et al. Strengthened Peening Effect on Metallurgical Bonding Formation in Cold Spray Additive Manufacturing[J]. Journal of Thermal Spray Technology, 2019, 28(4): 769-779.
- [24] HUANG Jian, MA Wen-hua, XIE Ying-chun, et al. Influence of Cold Gas Spray Processing Conditions on the Properties of 316L Stainless Steel Coatings[J]. Surface Engineering, 2019, 35(9): 784-791.
- [25] ZAHIRI S H, FRASER D, GULIZIA S, et al. Effect of Processing Conditions on Porosity Formation in Cold Gas Dynamic Spraying of Copper[J]. Journal of Thermal Spray Technology, 2006, 15(3): 422-430.
- [26] HUANG Jian, YAN Xing-chen, CHANG Cheng, et al. Pure Copper Components Fabricated by Cold Spray (CS) and Selective Laser Melting (SLM) Technology[J]. Surface and Coatings Technology, 2020, 395: 125936.
- [27] MA Wen-hua, XIE Ying-chun, CHEN Chao-yue, et al. Microstructural and Mechanical Properties of High-Performance Inconel 718 Alloy by Cold Spraying[J]. Journal of Alloys and Compounds, 2019, 792: 456-467.
- [28] GÄRTNER F, STOLTENHOFF T, VOYER J, et al. Mechanical Properties of Cold-Sprayed and Thermally Sprayed Copper Coatings[J]. Surface and Coatings Technology, 2006, 200(24): 6770-6782.
- [29] STOLTENHOFF T, BORCHERS C, GÄRTNER F, et al. Microstructures and Key Properties of Cold-Sprayed and Thermally Sprayed Copper Coatings[J]. Surface and Coatings Technology, 2006, 200(16/17): 4947-4960.
- [30] YU B, TAM J, LI W, et al. Microstructural and Bulk Properties Evolution of Cold-Sprayed Copper Coatings after Low Temperature Annealing[J]. Materialia, 2019, 7: 100356.
- [31] SUDHARSHAN PHANI P, VISHNUKANTHAN V, SUNDARARAJAN G. Effect of Heat Treatment on Properties of Cold Sprayed Nanocrystalline Copper Alumina Coatings[J]. Acta Materialia, 2007, 55(14): 4741-4751.
- [32] 章华兵. 冷喷涂粒子变形结合行为及涂层组织力学性能研究[D]. 上海: 上海交通大学, 2007.
- ZHANG Hua-bing. Research on Deformation, Deposition Behaviors of Particles and Microstructures, Mechanical Properties of Coatings in Cold Spray[D]. Shanghai: Shanghai Jiao Tong University, 2007.
- [33] 冯力, 李洞亭, 畅继荣, 等. 低压冷喷涂增材制造铜基块体性能研究[J]. 稀有金属材料与工程, 2020, 49(5): 1729-1735.
- FENG Li, LI Dong-ting, CHANG Ji-rong, et al. Properties of Copper-Based Bulks Materials Produced by Low Pressure Cold Spray Additives[J]. Rare Metal Materials and Engineering, 2020, 49(5): 1729-1735.
- [34] 侯江涛, 郝庆乐, 张雷, 等. 银铜合金再结晶过程组织性能演变研究[J]. 贵金属, 2019, 40(S1): 40-43.
- HOU Jiang-tao, HAO Qing-le, ZHANG Lei, et al. Study on the Evolution of Microstructure and Properties during Recrystallization of Ag-Cu Alloy[J]. Precious Metals, 2019, 40(S1): 40-43.
- 责任编辑: 刘世忠